Molecular Therapy
Oncolytics
Original Article

miR-301 regulates the SIRT1/SOX2 pathway via CPEB1 in the breast cancer progression

Yanjing Jia,[1,4] Jie Zhao,[2,4] Jinjie Yang,[3] Jie Shao,[1] and Zihao Cai[1]

[1]Department of General Surgery, Huashan Hospital, Fudan University, Shanghai 200040, PR China; [2]Department of Nursing, North Branch of Huashan Hospital, Fudan University, Shanghai 200040, PR China; [3]Shanghai MCC Hospital, Shanghai 201900, PR China

Breast cancer, the most common malignant tumor in women, has become a worldwide burden for family and society. MicroRNAs (miRNAs or miRs) are recognized as critical mediators of cancer-related processes, since they have the ability to coordinately suppress multiple target genes. In this study, we aim to find out specific miRNAs involved in the progression of breast cancer and explore the underlying molecular mechanism. Bioinformatics analysis suggested miR-301 as a differentially overexpressed miRNA in breast cancer, which was confirmed by expression determination. Functional assays were employed to explore the effect of miR-301 and its downstream effectors cytoplasmic polyadenylation element-binding protein 1 (CPEB1), SIRT1, and SOX2 on malignant phenotypes of breast cancer. The interaction among these factors was explained using luciferase and RNA immunoprecipitation (RIP) assays. In addition, the *in vivo* impact of miR-301 on breast cancer was assessed by cellular tumorigenicity in nude mice. We found that miR-301 overexpression restricted CPEB1 level and further promoted cell proliferation, metastasis, and cell cycle progression and impeded apoptosis. Moreover, CPEB1 regulated breast cancer development by mediating the SIRT1/SOX2 pathway. Further, miR-301 overexpression accelerated tumor formation in nude mice. Our results indicate that miR-301 overexpression accelerates the progression of breast cancer through the CPEB1/SIRT1/SOX2 axis.

INTRODUCTION

Breast cancer is the most common cancer in females with an increasing incidence rate throughout the globe.[1,2] Nearly 11% of the worldwide breast cancer cases occur in China, where it is the sixth-leading cause of cancer-related deaths among females.[3] However, such traditional therapies as surgical excision, hormone therapy, radiotherapy, and chemotherapy and surgical treatment are still accompanied by significant recurrence and metastasis.[4] It should be noted that the understanding of the mechanisms underlying the signaling pathways orchestrating tumorigenesis and metastasis in breast cancer have been extensively studied.[5]

Interestingly, the aberrant regulatory interaction of microRNA (miRNA)-mRNA that mediates the malignant phenotypes of cancer cells may provide novel targets and therapies to limit development of malignancies, including breast cancer.[6] miRNAs are small non-coding RNAs existing in both nucleus and cytoplasm, repressing gene expression by binding to their target mRNAs via complementary sequences of the 3′ untranslated region (3′ UTR).[7] Among different breast cancer subtypes, the specific miRNA signatures are shown as either oncogenes or tumor suppressor genes.[8] In the present study, differentially expressed miRNAs and their target genes related to breast cancer were predicted through bioinformatic analyses, where microRNA (miR)-301 and cytoplasmic polyadenylation element-binding protein 1 (CPEB1) were chosen for subsequent experiments. The involvement of miR-301 has been identified in a previous study by Shi et al.[9], which illuminated that the overexpression of miR-301 presented with a tumor-supporting role in cancer cell angiogenesis, tamoxifen resistance, and tumor growth. However, this study failed to clarify the specific downstream molecular mechanisms behind breast cancer progression. Furthermore, the oncogenic effect of miR-301 has also been explored in clinical samples in the study of Qui et al.,[10] where abnormally high expression of miR-301 has been associated with shorter overall survival of patients with breast cancer. Presently, there is only one study suggesting that miR-301 mediates breast cancer through transcriptional regulation of target mRNAs, including PTEN, FoxF2, BBC3, and Col2A1.[9] Still, the involved downstream regulatory signaling pathways have not been fully established. Notably, the metastatic potential of breast cancer cells to the lung was accelerated in response to CPEB1 depletion, but ectopic expression of CPEB1 halted the metastasis.[11] Therefore, it is reasonable to hypothesize that the regulation of miR-301 on CPEB1 may play a potential role in the development of breast cancer.

In the present study, we validated the expression of miR-301 in clinical samples, cell lines, and animal models of breast cancer. Further, functional experiments were performed to characterize the effect of

Received 7 September 2020; accepted 9 March 2021;
https://doi.org/10.1016/j.omto.2021.03.007.

[4]These authors contributed equally

Correspondence: Jie Shao, Department of General Surgery, Huashan Hospital, Fudan University, No. 12, Middle Wulumuqi Road, Jingan District, Shanghai 200040, PR China.
E-mail: drshaojie@163.com
Correspondence: Zihao Cai, Department of General Surgery, Huashan Hospital, Fudan University, No. 12, Middle Wulumuqi Road, Jingan District, Shanghai 200040, PR China.
E-mail: davidcai@139.com

miR-301 and its target CPEB1 in malignant phenotypes of breast cancer, as well as the involvement of the SIRT1/SOX2 signaling pathway. This current study intended to provide promising therapeutic targets for diagnosis and treatments of breast cancer.

RESULTS

Bioinformatics analyses

Analysis of GEO database breast cancer miRNA microarrays GEO: GSE26659, GSE45666, GSE44124, and GSE31309 by R language difference yielded 73, 110, 100, and 100 differentially expressed miRNAs, respectively. Subsequently, the upregulated miRNAs and downregulated miRNAs obtained from their analysis results were intersected, respectively (Figure 1A). We finally found that hsa-miR-301a and -miR-183 were significantly, highly expressed in all microarrays, and hsa-miR-145-3p was significantly lowly expressed in all microarrays. Figure 1B shows the expression heatmap of 50 differentially expressed genes including miR-301a in microarray GEO: GSE26659 (Figure 1B). miR-301a was found to be highly expressed in breast cancer by starBase (Figure 1C), and Kaplan-Meier (KM)-plotter analysis showed that the high expression of miR-301a significantly reduced the survival rate of breast cancer patients (Figure 1D), so miR-301a was selected as the object of subsequent studies. Further, the downstream genes of miR-301a were predicted by RAID, mirDIP, TargetScan, DIANATOOLS, and miRDB, with 394, 220, 10, 50, and 5 candidate target genes attained, respectively. Then, 3,554 differential genes were obtained by analyzing the breast cancer database in The Cancer Genome Atlas (TCGA) database using the online tool GEPIA, of which 2,133 genes were significantly lowly expressed in breast cancer, and the predicted miR-301a candidate target genes were intersected with the significantly downregulated genes in TCGA (Figure 1E), and finally the candidate target gene GPEB1 was obtained. Through TargetScan, we obtained the binding site map of miR-301a and CPEB1 (Figure 1F), searched the expression of CPEB1 in breast cancer by GEPIA, and found that it was a significantly lowly expressed gene (Figure 1G). The clinical data of CPEB1 expression and breast cancer recurrence-free survival (RFS) curve were drawn by the online tool KM-Plotter analysis, and decreased CPEB1 was found to be significantly reduced survival rate of breast cancer patients (Figure 1H). Further analysis of the expression correlation between miR-301a and CPEB1 in TCGA breast cancer revealed a significant negative correlation between them (Figure 1I). Previous studies indicated that CPEB1 can moderate the expression of SIRT1 [12], whereas SIRT1 can have an effect on the expression of SOX2.[13,14] Moreover, highly expressed SIRT1 was found in breast cancer.[15] Upregulated SOX2 was demonstrated to predict the poor prognosis of breast cancer.[16] Therefore, we proposed that miR-301a regulates the SIRT1/SOX2 pathway by changing the expression of CPEB1, which affects the occurrence of breast cancer.

miR-301 is highly expressed in breast cancer tissues and cells

In order to observe the expression of miR-301 in breast cancer, we first used qRT-PCR to gain the expression level of miR-301 in 85 breast cancer tissues and related para-cancerous tissues. Compared with para-cancerous tissues, the expression of miR-301 in breast cancer tissues was significantly higher (Figure 2A). Moreover, the level of miR-301 was positively related with the breast cancer stage (Figure 2B). Relationship between miR-301 expression level and clinicopathological parameters of breast cancer patients is shown in Table 1. Then, we calculated the median of the expression of miR-301 in 85 breast cancer tissues, which was used as a cutoff value for prognostic analysis. Patients with high miR-301 expression showed lower survival rate (Figure 2C). Further, we found that compared with the normal breast epithelial cell line MCF-10A, miR-301 had a higher expression level in three breast cancer cell lines: MCF-7, MDA-MB-231, and MDA-MB-468. Among them, the expression level of breast cancer cell line MCF-7 was the highest (Figure 2D), so we chose this cell line for transfection and follow-up related experiments.

miR-301 promotes the malignant phenotypes of breast cancer cells

Aimed to explore whether different expression of miR-301 can cause differences in biological functions of breast cancer cells, the breast cancer cell line MCF-7, obtained by the above screening process, was selected to detect its expression after being transfected. It was worth noting that the expression of miR-301 was higher after miR-301 mimic treatment but lower after miR-301 inhibitor treatment (Figure 3A), indicating that the vector was successfully transfected. Then, functional experiments demonstrated that miR-301 mimic treatment led to enhanced cell proliferation, migration, and invasion, as well as a decreased number of cells at the G0/G1 phase and apoptosis, whereas miR-301 inhibitor treatment caused the opposite trends (Figures 3B–3F). In addition, we gained the expression of MCM2, MMP2, caspase-3 and cleaved caspase-3 from qRT-PCR and western blot, respectively. As the results displayed, upregulated miR-301 increased the expression of MCM2, MMP2, and cleaved caspase-3 but decreased expression of caspase-3, whereas downregulation of miR-301 led to opposite trends (Figures 3G and 3H). To sum up, overexpression of miR-301 may promote the invasion, migration, and proliferation of breast cancer cells, accelerate the cell cycle, and inhibit apoptosis.

miR-301 targets CPEB1

A dual luciferase reporter gene experiment revealed that compared with the mimic-negative control (NC) group, luciferase activity of 3′ UTR of CPEB1-wild type (WT) was inhibited by miR-301, but the luciferase activity of 3′ UTR of CPEB1-mutant (mut) was not affected (Figure 4A). The results of an RNA immunoprecipitation assay (RIPA) (Figure 4B) indicated both miR-301 and CPEB1-WT bound by Ago2 were significantly increased compared with immunoglobulin G (IgG), indicating that miR-301 can specifically bind to the 3′ UTR region of CPEB1 and reduced CPEB1 gene expression at the post-transcriptional level. By using qRT-PCR, we found a low expression level of CPEB1 in breast cancer tissues (Figure 4C). Moreover, the negative correlation between miR-301 and CPEB1 was also found (Figure 4D). Then, by interfering with the expression of miR-301, we detected the protein and mRNA expression of CPEB1 in each group by western blot and qRT-PCR (Figures 4E–4G). As the results represented, the protein and mRNA expression of CPEB1 was

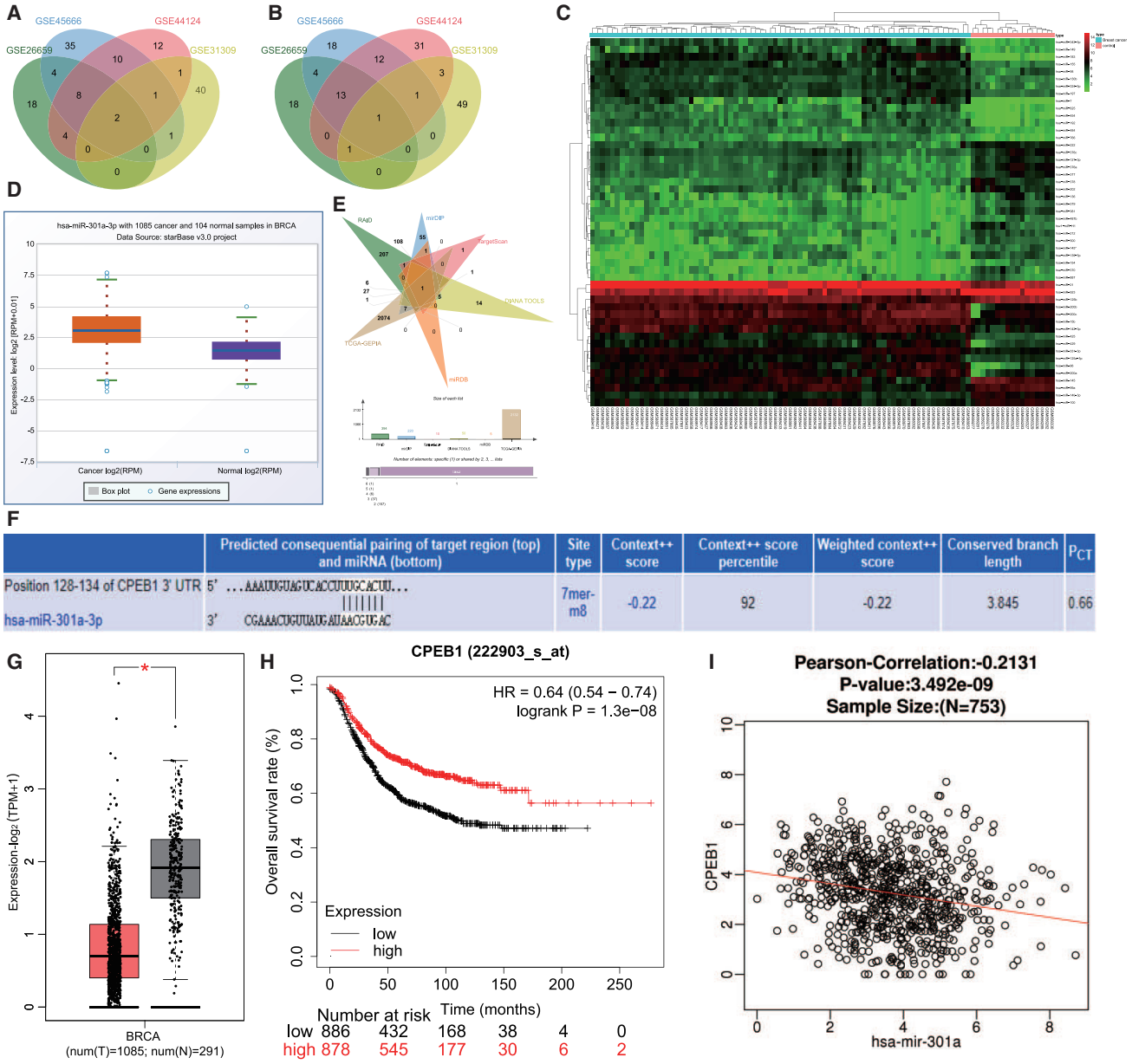

Figure 1. miR-301a is predicted to affect breast cancer by regulating CPEB1-mediated SIRT1/SOX2

(A) The Venn plot of differentially expressed miRNA obtained by analyzing the difference of breast cancer-related miRNA microarray dataset in GEO database; (B) The expression heatmap of 50 differentially expressed miRNA of microarray dataset GSE26659, and the color level is in the upper right corner; (C) The boxplots presenting the expression of miR-301a, the left one corresponds to breast cancer tissues, the right one corresponds to normal tissues (FDR=1.2e-22); (D) The survival curve of miR-301a in breast cancer. (E) The Venn map identifying the key downstream gene-CPEB1; (F) Map of binding sites of miR-130a and CPEB1 in TargetScan; (G) Expression Boxplots of CPEB1 in Breast Cancer in TCGA Database, the red box on the left corresponds to the breast cancer sample, and the gray box on the right corresponds to the normal sample, * $P < 0.05$, ($p = 3.17e-111$); (H) Based on TCGA database, the survival curve of the relationship between CPEB1 expression and breast cancer type and survival condition ($P = 2.5e-09$). (I) Correlation analysis between miR-301a and CPEB1 in breast cancer dataset included in TCGA, with person correlation coefficient and correlation p-value above.

significantly lower after miR-301 mimic treatment but increased after miR-301 inhibitor treatment. The above results suggested that CPEB1 was lowly expressed in breast cancer, which was a direct target for miR-301.

CPEB1 regulated by miR-301 inhibits the malignant phenotypes of breast cancer cells

In order to further study the effect of CPEB1 expression on the biological function of breast cancer cells, we designed three small

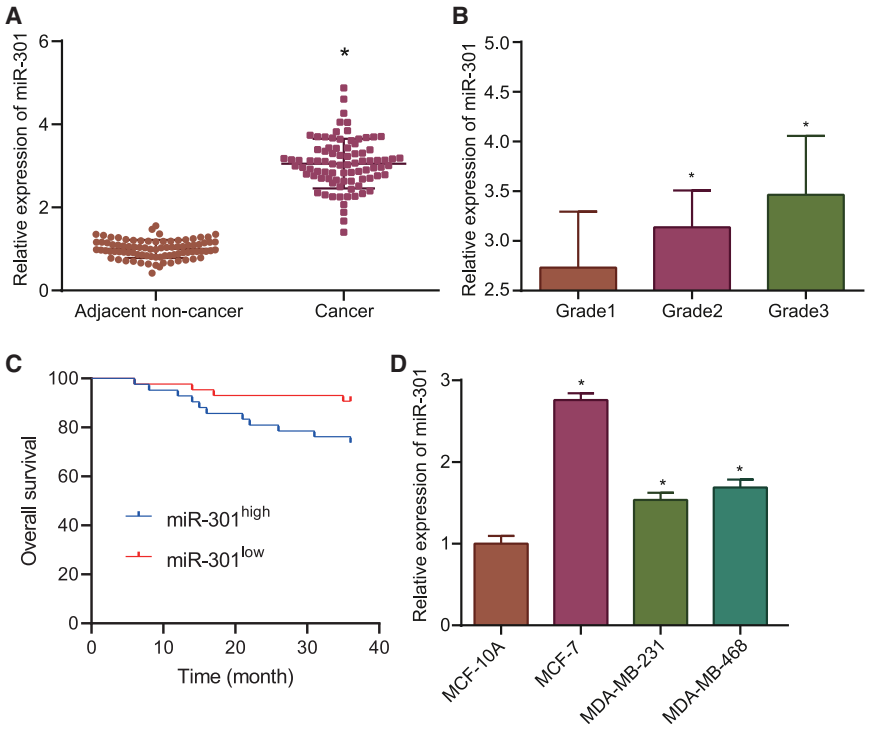

Figure 2. High expression of miR-301 in breast cancer

(A) Expression level of miR-301 in breast cancer and normal tissues. (B) Relative expression level of miR-301 in different stages of breast cancer. (C) Prognostic analysis based on the average expression level of miR-301 in breast cancer. (D) Expression of miR-301 in normal breast epithelial cell line and breast cancer cell line. The continuous variables were described by mean ± standard deviation. *$p < 0.05$ compared with normal tissues or normal breast epithelial cells. Paired sample t test, independent sample t test, or one-way analysis of variance (ANOVA) was conducted to test inter-group differences in continuous variables. Kaplan-Meier was used for survival analysis. N = 85. The experiment was performed three times.

interfering (si)-CPEB1 and selected the si-CPEB1_2 with the highest interference efficiency as the subject (Figure 5A). In the following, the interaction between miR-301 and CPEB1 in breast cancer cell functions was investigated. It was found that downregulated CPEB1 induced cell proliferation, migration, and invasion, as well as led to a decreased number of cells at the G0/G1 phase and apoptosis; they were reversed by the miR-301 inhibitor (Figures 5B–5F). Additionally, we detected the relative expression levels of proliferation-related factor MCM2, migration- and invasion-related factors MMP2, apoptosis-related factors caspase-3, cleaved caspase-3 in each group by qRT-PCR, and western blot, respectively (Figures 5G and 5H). We found that the relative expression levels of mRNA and protein of MCM2 and MMP2, as well as cleaved caspase-3 expression, were significantly higher, but that of caspase-3 was significantly decreased after si-CPEB1, whereas they were reversed by the addition of the miR-301 inhibitor. Together, decreased miR-301 could suppress malignant phenotypes of breast cancer cells by increasing CPEB1.

CPEB1 regulates the SIRT1/SOX2 pathway in the development of breast cancer

Previous studies confirmed that CPEB1 can modulate the methylation status and translation process of SIRT1,[12] and SIRT1 can affect the related biological functions of hepatocellular carcinoma cells through SOX2 at the transcription level.[13] In order to identify the mechanism of the effect of CPEB1 on breast cancer, first, qRT-PCR was performed to determine the expression of SIRT1 and SOX2 in breast cancer. The results revealed that SIRT1 and SOX2 were highly expressed in breast cancer tissues (Figure S1). Besides, we verified the targeting relationship between CPEB1 and SIRT1 by using a dual luciferase reporter gene experiment (Figure 6A). Compared to the si-NC group, the luciferase activity of 3′ UTR of SIRT1-WT of the si-CPEB1 group was stronger, but the luciferase activity of 3′ UTR of SIRT1-mut was not influenced. Moreover, expression determination of SIRT1 by qRT-PCR and western blot revealed that decreased CPEB1 elevated SIRT1 protein expression but showed no change in mRNA expression of SIRT1 (Figures 6B and 6C). RIPA showed that both CPEB1 and SIRT1 bound by Ago2 were significantly increased compared with IgG, indicating that CPEB1 combined to the 3′ UTR region of SIRT1 specifically and reduced the expression of SIRT1 after transcription (Figure 6D). Subsequently, after si-SIRT1 transfection, the expression of SIRT1 and SOX2 was tested by qRT-PCR and western blot with the results showing that decreased SIRT1 reduced protein and mRNA expression of SIRT1 and SOX2, whereas the addition of si-CPEB1 increased protein expression of SIRT1 and SOX2 but exerted no effect on mRNA expression of SIRT1 and SOX2 (Figures 6E and 6F).

To identify whether the biological functions of breast cancer cells can be affected by the expression of SIRT1, Cell Counting Kit-8 (CCK-8), Transwell, and flow cytometry were performed. It was found that si-SIRT1 caused decreased cell proliferation, migration, and invasion, as well as led to an increased number of cells at the G0/G1 phase and apoptosis; those changes were reversed by si-CPEB1 (Figures 6G–6K). Additionally, qRT-PCR and western blot demonstrated that si-SIRT1 caused decreased MCM2, MMP2, and cleaved caspase-3 expression but increased caspase-3 expression, whereas the addition of si-CPEB1 led to opposite trends (Figures 6L and 6M). Meanwhile, to demonstrate the link between miR-301 and the CPEB1/SIRT1/SOX2 pathway, we overexpressed (oe)-SIRT1 after knockdown of miR-301 in MCF-7 cells and detected cell proliferation by the CCK-8 assay, and the results showed that the decreased cell proliferation induced by miR-301 could be blocked by highly expressed SIRT1 (Figure 6N), and similar results also appeared in cell migration and invasion assays (Figures 6O and 6P)

Table 1. Relationship between miR-301 expression level and clinicopathological parameters of breast cancer patients

Variable	Number of cases	High miR-301	Low	p
Grade				
1	36	12	24	0.05
2	26	13	13	
3	23	17	6	
Molecular phenotype				
Luminal A	38	12	26	0.05
Luminal B	16	9	7	
Triple negative	18	13	5	
HER2	13	8	5	

We could conclude from these results that low expression of CPEB1 activated the SIRT1/SOX2 pathway to increase the ability of invasion, migration, and proliferation of breast cancer cells, promote cell cycle progression, and inhibit apoptosis, confirming the important role of the miR-301/CPEB1/SITR1/SOX2 pathway in regulating breast cancer cell proliferation, migration, and invasion.

miR-301 promotes the tumorigenicity of breast cancer cells *in vivo*

In order to study the influence of miR-301 on tumor formation, the stably transfected breast cancer cells were injected into nude mice subcutaneously, and the tumor volume was measured after a period of time. The results (Figures 7A and 7B) presented in the tumor volume increased gradually, and the average tumor volume and average tumor weight of mice bearing cells expressing miR-301 mimic were bigger, whereas miR-301 inhibitor treatment led to opposite trends. At the same time, if SIRT1 levels were rescued, then both the volume and weight of the tumor would revert to levels similar to those of the inhibitor-NC group. Results from immunohistochemistry presented that the miR-301 mimic resulted in decreased CPEB1 expression but increased SIRT1 and SOX2 expression, whereas miR-301 inhibitor treatment led to opposite trends in tumors (Figure 7C). The obtained results from immunohistochemistry were also confirmed by western blot (Figure 7D). TUNEL assay indicated that mice-bearing cells expressing the miR-301 mimic had a lower apoptosis rate, whereas mice-bearing cells expressing the miR-301 inhibitor showed a higher apoptosis rate (Figure 7E). In conclusion, the higher expression of miR-301 reduces the expression level of CPEB1, then regulated the SIRT1/SOX2 pathway, and finally promoted the tumorigenicity of breast cancer cells *in vivo*.

DISCUSSION

Breast cancer is one of the most frequently diagnosed fatal cancers and the leading cause of cancer-related death among women.[17] It has been noted that miRNAs have the ability to modulate gene expression associated with tumor etiology and development of variable malignancies including breast cancer, which may offer clues for improved understanding of underlying molecular mechanisms.[18] In the present study, a previously unrecognized mechanism of miR-301-induced breast cancer progression was shown, which was achieved through the downregulation of CPEB1 and the mediation of the SIRT1/SOX2 signaling pathway.

We validated that highly expressed miR-301 was associated with an unfavorable prognosis in patients with breast cancer. These findings suggested that miR-301 may act as an oncomiR augmenting breast cancer progression. Then, we also revealed that miR-301 presented with higher expression in breast cancer cell lines relative to normal mammary epithelial cells, whereas the MCF-7 cell line had the highest expression. Consistently, miR-301 has been reported to play key roles in the proliferation and invasion of human breast cancer cells,[9] and miR-301 could mediate the nuclear factor κB (NF-κB) and PTEN/Akt pathways vital to the development of breast cancer.[19] Moreover, we showed the overexpression of miR-301 facilitated breast cancer cell proliferation, migration, invasion, and cell cycle entry, while inhibiting cell apoptosis. This finding corroborates that of a previous study, which demonstrated that ectopically expressed miR-301 caused significant elevations in invasive and migratory potential of breast cancer cells.[9] Meanwhile, emerging evidence has proposed the tumor-initiating activities of miR-301 in a wide array of human malignancies, such as malignant melanoma,[20] esophageal squamous cell carcinoma,[21] and non-small cell lung cancer.[22] In addition, miR-301 functions through mediating different mRNAs among different cancer types. For instance, miR-301 may mediate breast cancer tumorigenesis by directly targeting PTEN, FoxF2, BBC3, and Col2a1.[9] Besides, the promotive role of miR-301 in gastric cancer was linked with the binding affinity to ZBTB4, and miR-301-mediated ZBTB4 inhibition accelerated the tumor progression in gastric cancer.[23] Still, there is little evidence clarifying the how miR-301 serves as an oncomiR in breast cancer.

The present study hence proceeded to probe into the specific relationship between miR-301 and CPEB1 and predicted the putative binding affinity through *in silico* analyses. The dual luciferase reporter gene assay further validated that miR-301 targeted and downregulated the expression of CPEB1. Additionally, it was observed that the expression level of CPEB1 was negatively correlated with poor prognosis of patients with breast cancer. There is a paucity of evidence reporting that CPEB1 could modulate the balance between senescence and proliferation, playing a pivotal role in cancer development.[12,24,25] Moreover, it was also demonstrated by the current study that miR-301 knockdown upregulated the CPEB1 expression, which subsequently restrained breast cancer cell migration and invasion and enhanced cell apoptosis. Consistently, CPEB1 has been described as a tumor repressor regulated by miRNAs, such as miR-183 in endometrial cancer[26] and miR-455-5p in melanoma.[27] These observations support our study that miR-301 facilitated breast cancer cell proliferation through downregulating CPEB1, which acted as a tumor suppressor restricting tumorigenesis.

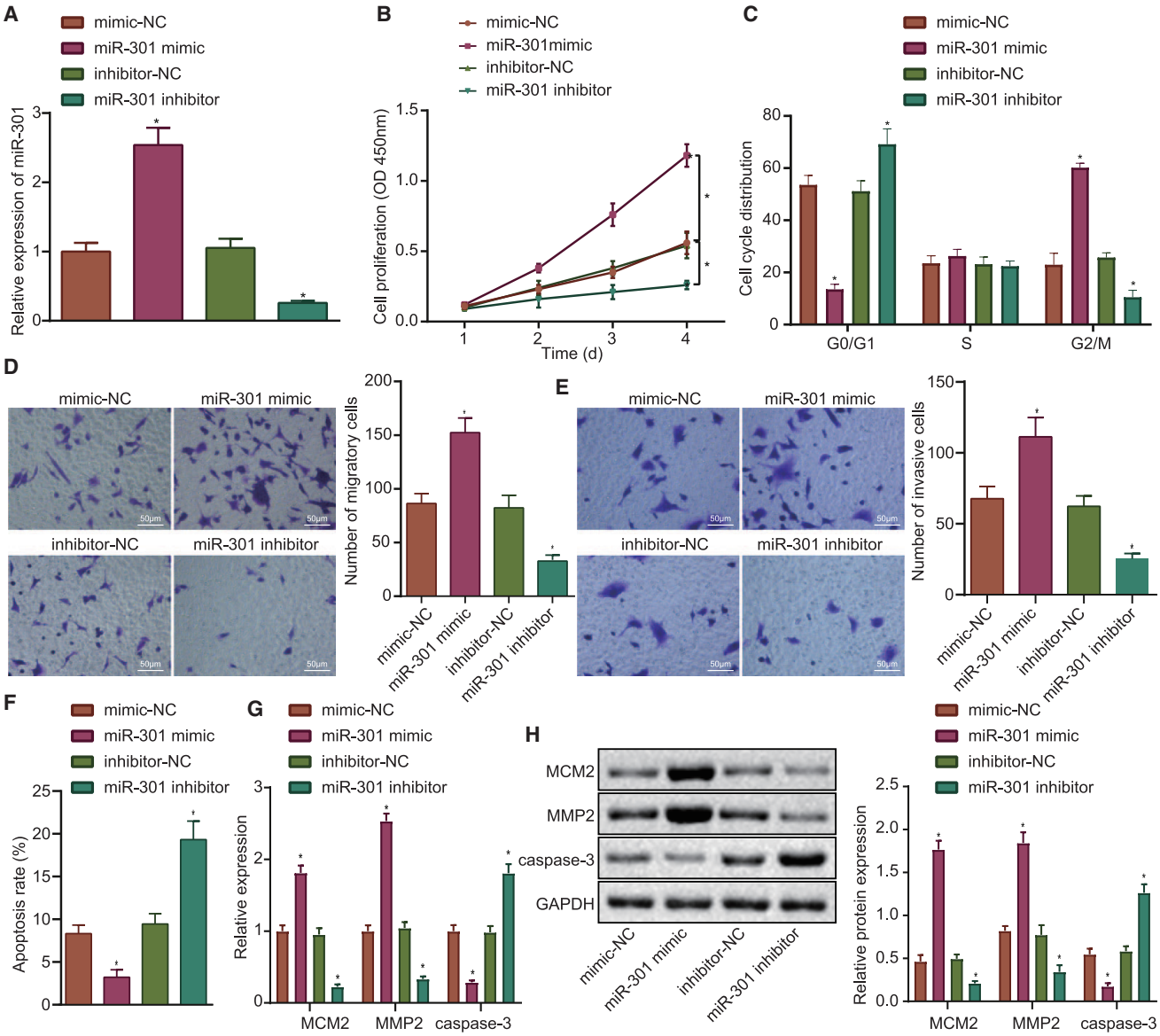

Figure 3. High expression of miR-301 can promote the invasion and proliferation of breast cancer cells as well as inhibit their apoptosis

(A) Detection of miR-301 expression level by qRT-PCR. (B) Detection of breast cancer cell proliferation by CCK-8. (C) Distribution chart of breast cancer cell cycle. (D) Detection of migration ability of breast cancer cells by Transwell. (E) The relative number of invasive breast cancer cells, as measured by Transwell assay. (F) Apoptosis rate of breast cancer cells. (G) Detection of mRNA expression level of proliferation-related factor MCM2, migration- and invasion-related factors MMP2, and apoptosis-related factors caspase-3 by qRT-PCR. (H) Detection of protein expression level of proliferation-related factor MCM2, migration- and invasion-related factors MMP2, and apoptosis-related factors caspase-3 by western blot. The continuous variables were expressed by mean ± standard deviation. *$p < 0.05$ compared with the NC group. Paired sample t test, independent sample t test, or one-way ANOVA was selected to test the inter-group differences of continuous variables. The difference of data of each group at different times was analyzed by two-way ANOVA. We repeated the experiment three times in order to obtain accurate and stable results.

Further mechanistic investigation unraveled the implication of the SIRT1/SOX2 signaling pathway in miR-301-mediated CPEB1 in breast cancer. At present, a few studies suggested that CPEB1 might repress the expression of SIRT1 to modulate cancer stemness in glioma[28] and hepatocellular carcinoma,[12] but how CPEB1 interacts with SIRT1 in breast cancer still remains to be determined. The role of SIRT1 in cancer is still under debate.[29,30] Another previously conducted study considered SIRT1 as a tumor suppressor involved in DNA damage response.[31] More importantly, the pro-tumorigenic role of SIRT1 in breast cancer, lung carcinoma, and prostate cancer has been demonstrated.[32] In this study, we confirmed that CPEB1 could bind to 3′ UTR of SIRT1 and repressed SIRT1 protein

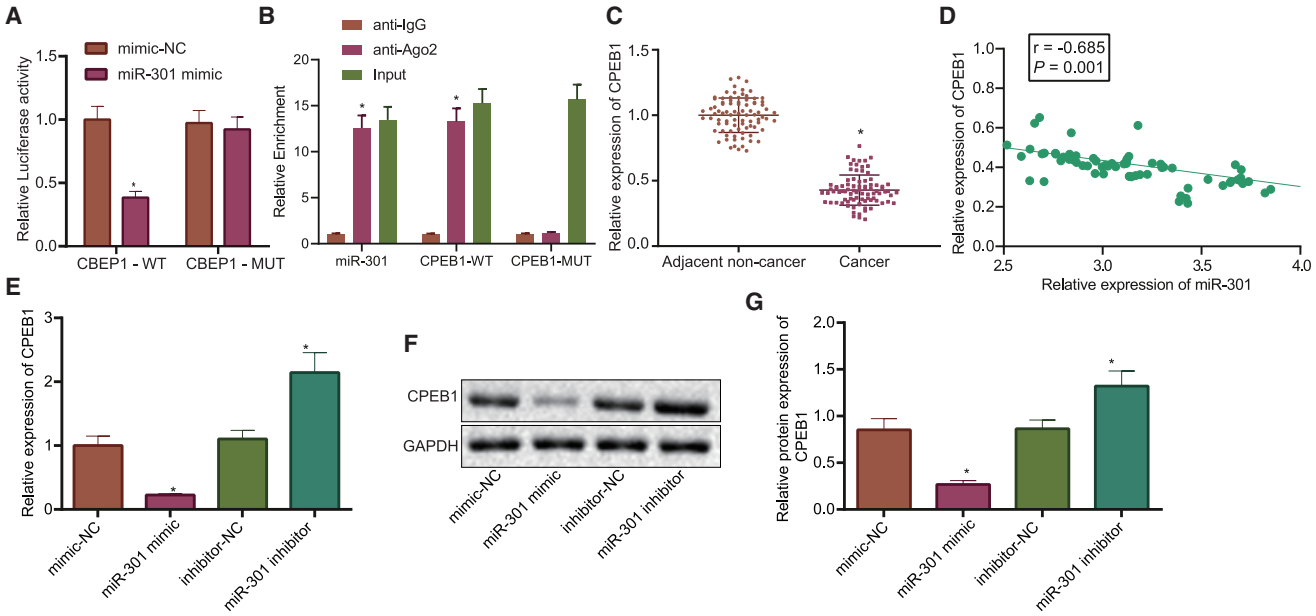

Figure 4. Targeted regulation of CPEB1 expression by miR-301

(A) Detection results of fluorescence activity of miR-301 and CPEB1. (B) RIP experiment to detect the combination of miR-301, CPEB1, and Ago2. (C) Detection of CPEB1 expression in cancer and para-cancerous tissues by qRT-PCR. (D) Correlation analysis of miR-301 and CPEB1. (E) The expression of CPEB1 in each group of cells was tested by qRT-PCR. (F) Protein bands of CPEB1 in each group of cells. (G) Western blot was used to detect the protein expression of CPEB1 in each group of cells. The continuous variables were expressed by mean ± SD (standard deviation). *$p < 0.05$ compared with normal tissues or normal cells. Paired sample t test, independent sample t test, or one-way ANOVA was used to compare the differences of continuous variables among different groups. Pearson correlation is used to analyze the correlation between CPEB1 and miR-301. We repeated the experiment three times to get accurate and stable results.

expression in breast cancer cells. Furthermore, we revealed that SIRT1 knockdown repressed breast cancer cell proliferation, migration, and invasion, blocking cell cycle and promoting cell apoptosis, implying that SIRT1 functions as a tumor promoter in breast cancer cells. Moreover, several recent studies claimed the overexpression of SIRT1 in breast cancer, facilitating tumor growth and inhibiting cancer cell apoptosis,[32,33] which is in agreement with our findings. Notably, it has been suggested in hepatocellular carcinoma cancer that SIRT1 mediates the cell self-renewal through transcriptional regulating SOX2,[12,13] and SOX2 overexpression promoted cell adhesion in MCF-7 breast cancer cells.[34] Our results delineated that SIRT1 could modulate expression of SOX2, which was also upregulated in cells in the presence of CPEB1 knockdown, indicating that CPEB1 suppressed the expression of both SIRT1 and SOX2 and thus restrained breast cancer progression. Thus, CPEB1 may be a significant tumor suppressor in breast cancer by post-transcriptional regulating the SIRT1/SOX2 signaling pathway. Moreover, we also verified the mechanism of the inhibitory role of miR-301-mediated CPEB1/SIRT1/SOX2 signaling in nude mice with xenografted breast cancer.

Cumulatively, the main findings of this study indicated that miR-301 inhibits CPEB1 expression, which in turn upregulates SIRT1/SOX2 to enhance breast cancer progression (Figure 8). The current study provides promising therapeutic targets for diagnosis and treatments in breast cancer. Future studies may be performed to test the feasibility for miR-301 to be clinically applied as an early diagnostic biomarker and for miR-301 to be pharmacologically manipulated for breast cancer management.

MATERIALS AND METHODS

Bioinformatics

The "limma" package of the R language (http://www.bioconductor.org/packages/release/bioc/html/limma.html) was used to perform differential expression analysis of the breast cancer-related miRNA microarray databases GEO: GSE26659 (|log fold change [logFC]| > 1.5, $p < 0.01$), GSE45666 (|logFC| > 1.5, $p < 0.01$), GSE44124 (100 miRNA with the lowest p value), and GSE31309 (100 miRNA with the lowest p value) retrieved from the GEO database (https://www.ncbi.nlm.nih.gov/gds). Then, miRNA with significant differences was screened and obtained. The key miRNA was obtained by drawing a Venn map and taking the intersections, and the expressional heatmap of the differential miRNAs was gained from GEO: GSE26659 (GEO: GSE26659 microarray database had 94 samples, including 17 normal samples and 77 breast cancer samples; GEO: GSE45666 microarray database had 116 samples in total, which included 15 normal samples and 101 breast cancer samples; GEO: GSE44124 microarray database had 53 samples, including 3 normal samples and 50 breast cancer samples; and GEO: GSE31309 microarray database had 106 samples in total, which included 57 normal samples and 48 breast

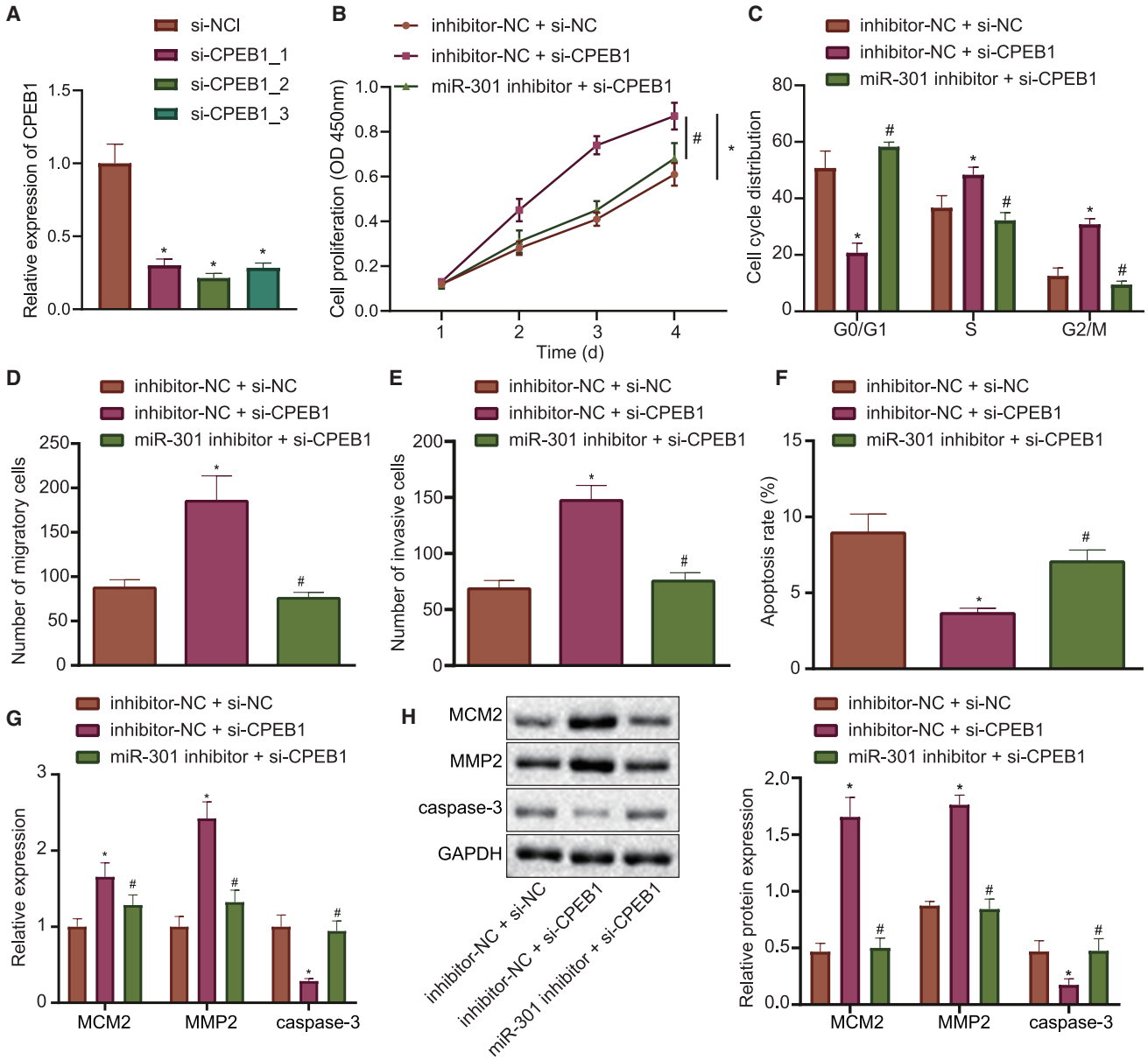

Figure 5. Low expression of miR-301 promotes the expression of CPEB1, thus inhibiting MCF-7 cell proliferation, migration, and invasion

(A) Expression of CPEB1 detected by qRT-PCR. (B) Detection of breast cancer cell proliferation by CCK-8. (C) Distribution of breast cancer cell cycle. (D) The relative number of migrating cells of breast cancer cells, as detected by Transwell. (E) The relative number of invasive cells of breast cancer cells. (F) Apoptosis rate of breast cancer cells. (G) The mRNA expression level of proliferation-related factor MCM2, migration- and invasion-related factors MMP2, and apoptosis-related factors caspase-3 was detected by qRT-PCR. (H) The protein expression of proliferation-related factor MCM2, migration- and invasion-related factors MMP2, and apoptosis-related factors caspase-3 was detected by western blot. The continuous variables were expressed by mean ± standard deviation. *$p < 0.05$ compared with the inhibitor-NC + si-NC group; #means compared with the inhibitor-NC + si-CPEB1 group. Paired sample t test, independent sample t test, or one-way ANOVA was used to compare the differences of continuous variables among different groups. Two-way ANOVA was selected to test the difference of cell activity in different groups at different times. The experiment was repeated three times.

cancer samples). Additionally, the starBase website was used to analyze the clinical data of breast cancer in TCGA database (https://portal.gdc.cancer.gov/) for the key survival curve and expression trend. The miRNA, which was most associated with the survival of breast cancer, was selected for further experiments of the current study. Several databases including the RAID (score > 0.65) (http://www.rna-society.org/raid2), mirDIP (integrated score > 0.85) (http://ophid.utoronto.ca/mirDIP/), TargetScan (the 10 genes with the lowest cumulative weight) (http://www.targetscan.org/vert_71/), DIANA Tools (the top 50 genes at miRNA-targeted gene [miTG]

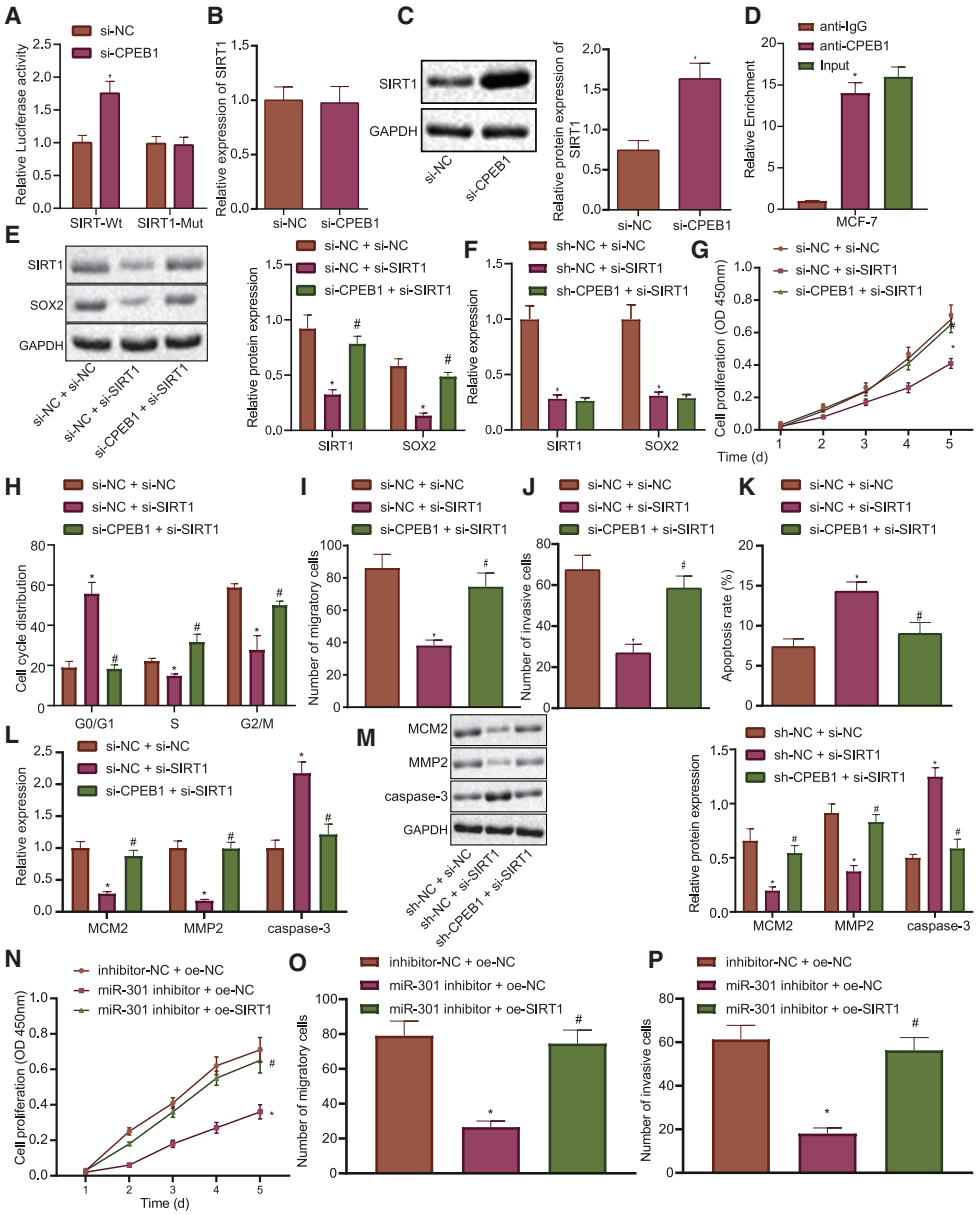

Figure 6. CPEB1 affects the occurrence and development of breast cancer by regulating the SIRT1/SOX2 pathway

(A) The results of fluorescence activity detection of CPEB1 and SIRT1. (B) The relative expression level of SIRT1 in each group of cells detected by qRT-PCR. (C) The protein expression level of SIRT1 in each group was detected by western blot. (D) The combination of CPEB1 and SIRT1 detected by a coimmunoprecipitation (coIP) experiment. (E) The protein expression of SIRT1 and SOX2 in cells of each group was detected by western blot. (F) The relative expression levels of CPEB1 and SOX2 in each group of cells were detected by qRT-PCR. (G) Proliferation of breast cancer cells detected by CCK-8. (H) Distribution of breast cancer cell cycle. (I) The relative number of migrating cells of breast cancer cells, as measured by Transwell. (J) The relative number of invading cells of breast cancer cells, as measured by Transwell. (K) Apoptosis rate of breast cancer cells. (L) mRNA expression level of related factors detected by qRT-PCR. (M) Protein expression level of related factors detected by western blot. (N) The proliferation of breast cancer cells after miR-301 knockdown and overexpression of SIRT1 detected by CCK-8 assay. (O) The migration ability of breast cancer cells after miR-301 knockdown or SIRT1 overexpression detected by Transwell assay. (P) The invasion ability of breast cancer cells after miR-301 knockdown or SIRT1 overexpression detected by Transwell assay. The continuous variables were expressed by mean ± standard deviation. *p < 0.05 compared with the si-NC + si-NC group; #means compared with the si-NC + si-SIRT1 group. Paired sample t test, independent sample t test, or one-way ANOVA was used to compare the differences of continuous variables among different groups. Two-way ANOVA was used to compare the data of cell activity among different groups at different time points. The experiment was repeated three times.

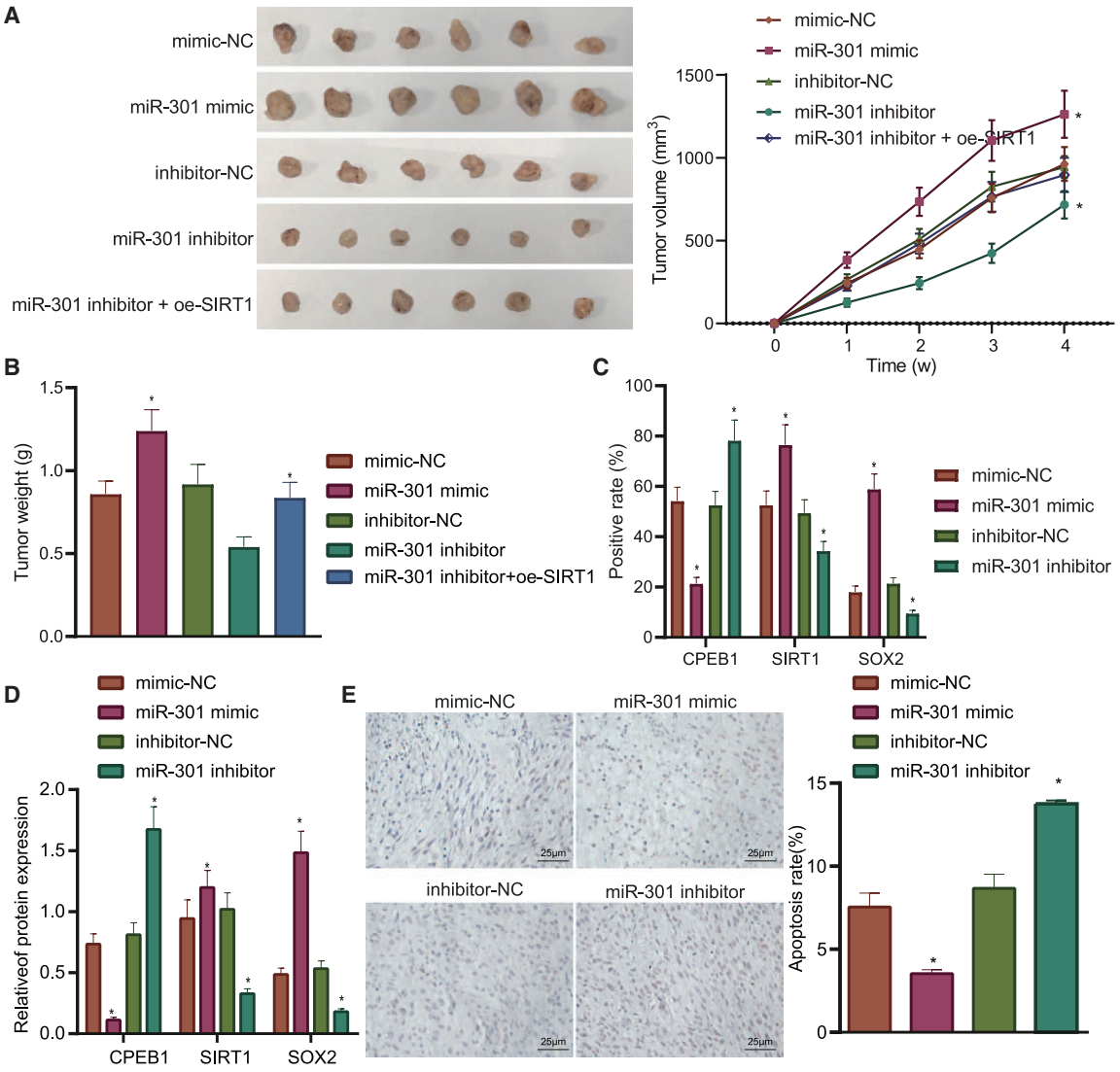

Figure 7. Higher expression level of miR-301 accelerates the process of tumor formation from breast cancer cells

(A) Tumor volume of the xenograft tumor in nude mice on day 28. (B) Tumor weight. (C) The expression of CPEB1, SIRT1, and SOX2 was detected by immunohistochemistry. (D) Protein expression of CPEB1, SIRT1, and SOX2 detected by western blot. (E) Detection of apoptosis by TUNEL staining (×400). The continuous variables were expressed by mean and standard deviation. *$p < 0.05$ compared with the NC group. Independent samples t test was selected for inter-group comparison; repeated-measures ANOVA was used to analyze the changing trend of tumor volume with time. The whole experiment was performed three times.

score) (http://diana.imis.athena-innovation.gr/DianaTools), and miRDB (target score = 100) (http://www.mirdb.org/) were used to forecast and filter the downstream target genes of miR-301a. Furthermore, the differentially expressed genes of breast cancer were obtained by analyzing the gene expression data of breast cancer in TCGA by the online tool GEPIA ($|logFC| > 1$, $p < 0.01$) (http://gepia.cancer-pku.cn/). The key downstream target genes were obtained by taking the intersection of the predicted target genes and the differentially expressed genes. The maps showing the binding sites among the miRNA genes were obtained using the TargetScan; co-expression analysis of miR-301a with CPEB1 in TCGA breast cancer was conducted through the starBase database; and the boxplots about the expression of key downstream genes in breast cancer were also created by GEPIA to get the expressional trend. The online tool "KM-Plotter" (http://kmplot.com/analysis/index.php?p=background) was utilized to analyze the relationship between gene expression level and breast cancer RFS curve. Then we looked for downstream regulatory pathways of key target genes by consulting the literature.

Patient enrollment

In the time span of June 2015 to June 2016, 85 breast cancer tissues and 85 para-cancerous tissues were collected from breast cancer

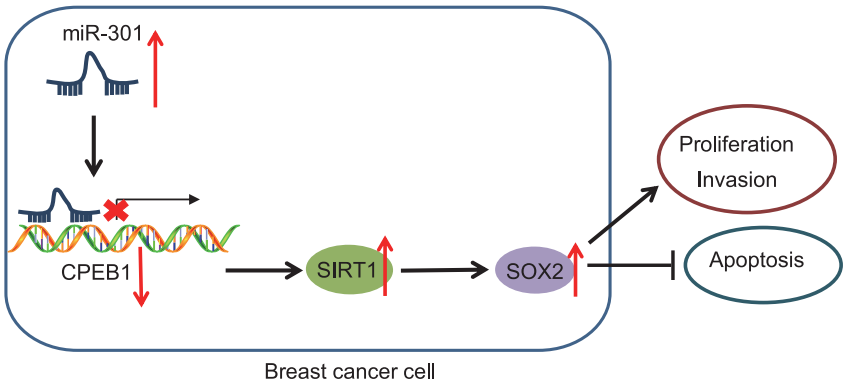

Figure 8. Schematic map of miR-301 in breast cancer
miR-301 overexpression accelerates the progression of breast cancer through the CPEB1/SIRT1/SOX2 axis

patients who had undergone surgical resection at Huashan Hospital, Fudan University. All of the samples were obtained from female patients (25−68 years) whose average age was 46.01 ± 10.27. Among all the patients, there were 36 patients at grade 1, 26 patients at grade 2, and 23 patients at grade 3. The inclusion criteria were as follows: (1) patients with invasive ductal carcinoma (IDC) type breast cancer; (2) patients with age ≥ 20 years old; and (3) patients with I−IV stage, according to American Joint Committee on Cancer (AJCC) diagnostic criteria. The exclusion criteria were as follows: (1) patients with a history of being diagnosed with other malignant tumors; (2) patients with other severe infections; (3) patients with cognitive impairment; and (4) patients with poor compliance or inability to understand the research process. All of the subjects did not necessarily receive adjuvant therapy, radiotherapy, or chemotherapy prior to the operation. Subsequently, the collected samples were divided into two parts. The first part was immediately stored in liquid nitrogen (−80°C) for the future extraction of RNA and proteins. After being fixed with paraformaldehyde and embedded in paraffin, the other part was ready for the subsequent experiments. Furthermore, patient follow-ups were conducted via telephone call and review. The follow-up was conducted 6−36 months after the study. Moreover, the follow-up period ended on June 30, 2019, and 80 patients had a complete follow-up, with an effective rate of 94.12% eventually. The current study's design gained the approval from the Institutional Review Board of Huashan Hospital, Fudan University. Each participant provided an informed consent form.

Cell culture

Human breast cancer cell lines MCF-7, MDA-MB-231, and MDA-MB-468 and normal mammary epithelial cell line MCF-10A were purchased from iCell Bioscience (Shanghai). Among them, MCF-7, MDA-MB-231, and MDA-MB-468 cells were cultured with the medium containing 90% RPMI 1640 and 10% fetal bovine serum (FBS). MCF-10A was cultured in DMEM/HAM F12 medium. All cell lines were cultured in a 5% CO_2 cell incubator at 37°C and screened by qRT-PCR.

Cell treatment

The breast cancer cells in the logarithmic phase were transfected with miR-301 mimic, miR-301 inhibitor, si-CPEB1, si-SIRT1, overexpression SIRT1, as well as their corresponding controls (mimic NC, inhibitor NC, and si-NC), according to the instructions of Lipofectamine (Invitrogen, USA). After transfection for 24 h, cells were collected, and the protein and RNA were extracted for expression determination. miR-301 mimic, miR-301 inhibitor, and their NCs were purchased from ABM (Applied Biological Materials). si-CPEB1, si-SIRT1, and their NCs were purchased from Sangon Biotech (Shanghai). The sequences are shown in Table S1.

qRT-PCR

Trizol (15596026; Invitrogen, Carlsbad, CA, USA) was used to extract the primary total RNA, and then RNA was reversely transcribed into cDNA, according to the guideline of PrimeScript RT Reagent Kit (RR047A; Takara, Japan). The method for determining primary transcripts of miRNA301a was used for miR-301. The primers of miR-301, CPEB1, MCM2, MMP2, SIRT1, caspase-3, U6, and glyceraldehyde 3-phosphate dehydrogenase (GAPDH) were designed by Sangon Biotech (Shanghai) (Table S2). The reaction solution was taken for real-time fluorescence quantitative PCR operation. The reaction system was 20 μL: 10 μL SYBR Premix, 2 μL cDNA template, 0.6 μL upstream primers, 0.6 μL downstream primers, and 6.8 μL DEPC water. The qRT-PCR experiment was carried out by using the 7500 fluorescent quantitative PCR. The $2^{-\triangle\triangle Ct}$ represents a multiple ratio of target gene expression in experimental and control groups. miR-301 was normalized to U6, and other genes were normalized to GAPDH.

Western blot

Cells after 24 h of transfection were lysed by RIPA pyrolysis solution containing 1 mM phenylmethylsulfonyl fluoride. Protein quantification was performed with Bio-Rad DC Protein Assay Kit (Guangzhou Yuwei Biotechnology Instrument). After protein separation through SDS-polyacrylamide gel electrophoresis, the protein was transferred from the gel to a polyvinylidene fluoride (PVDF) membrane. Next, the membrane was blocked in 1 × TBST containing 5% skim milk powder for 2 h at room temperature to block the non-specific binding site, followed by incubation with the following primary antibodies: CPEB1 (Affinity Biosciences; DF2462, rabbit antibody), MCM2 (Affinity Biosciences; AF0206, rabbit antibody), MMP2 (Affinity Biosciences; AF5330, rabbit antibody), and caspase-3 (Affinity Biosciences; AF6311, rabbit antibody). After that, the membrane was reprobed with secondary antibody IgG (Affinity Biosciences; S0001, goat anti-rabbit) for 1 h at room temperature. The development was done by using enhanced chemiluminescent (ECL) substrate. The gray values of western blot experimental protein expression

were measured by ImageJ software (NIH free software), and the experiment was carried out three times.

CCK-8 assay

CCK-8 Cell Proliferation and Toxicity Test Kit (C0038; Shanghai Biyuntian Biotechnology, PR China) was applied for a cell proliferation test. Cells were inoculated in 96-well plate (2,000 cells per well/100 μL medium), and 10 μL CCK-8 reagent was added to the corresponding well after transfection. The cells were incubated at 37°C for 2 h. The wells with only the corresponding amount of medium and CCK-8 reagent were used as blank control, and the absorbance values of each well at 450 mm wavelength were measured on the enzyme-labeling instrument. The value was proportional to the number of cell proliferation in the medium, and then the cell growth curve was drawn.

Transwell assay

In 250 μL serum-free medium, 3 × 10 ∼4 cells per well were pretreated with lycorine and added to the upper chamber. Then, the fresh medium containing 10% FBS was placed in the lower chamber, and the cells were incubated (37°C and 5% CO_2) for 24 h for migration determination. For invasion determination, the procedure was the same as above, except that the insert was coated with 200 mg/mL Matrigel. After 48 h of incubation, the migratory and invasive cells in the lower chamber were stained by 0.1% crystal violet. The images of breast cancer cells were taken under a phase contrast microscope; the experiments were conducted three times.

Flow cytometry

An annexin V-fluorescein isothiocyanate (FITC)/propidium iodide (PI) double-staining kit (KA3805; Abnova, USA) was selected to observe the apoptosis of breast cancer cells 48 h after transfection. Briefly, the cells of each group were centrifuged at 2,000 rpm for 5 min, re-suspended in pre-cool 1 × PBS, centrifuged at 200 rpm for 5−10 min, and added with 300 μL 1 × binding buffer for cell suspension. Next, the cells were added with 5 μL Annexin V-FITC for cultivation for about 15 min at room temperature in the absence of light. 5 min before flow cytometry (Cube 6; Partec, Germany), 5 μL of PI was added into cells for incubation for 5 min in the absence of light. When the excitation wavelength was 480 nm and 530 nm, FITC was detected. When the wavelength was greater than 575 nm, the PI was detected.

The cells of each group after transfection were collected, digested with 0.25% trypsin to make a single-cell suspension, washed twice with PBS, and centrifuged with the supernatant discarded. Next, the cells were treated with precooled 70% ethanol at 4°C overnight, re-suspended, centrifuged, and washed with pre-cooled PBS two times. The cells were re-suspended in 100 μL of PBS and added with RNase (final concentration: 1 mg/mL) for treatment for 30 min at 37°C. Then the cells were stained with PI staining solution (final concentration: 50 μg/mL) at 4°C for 40 min under the condition of avoiding light and washed with PBS followed by detection of the content of DNA in the cell cycle at an excitation wavelength of greater than 575 nm to calculate the percentage of cell cycle.

Dual luciferase assay

The biological prediction website was used to analyze the binding sites of miR-301 and CPEB1 and obtain the fragment sequences containing the acting sites. The 3′ UTR and mut 3′ UTR regions of CPEB1 and SIRT1 were cloned and amplified into the pmirGLO (E1330; Promega-Magna, USA) Luciferase carrier was named as pWT-CPEB1 and pmut-CPEB1 (binding site of miR-301 in CPEB1 3′ UTR: 5′-ACUG CACUC-3′; mut sequence: 5′-AAUGAACUU-3′) and pWT-SIRT1 and pmut-SIRT1 (binding site of CPEB1 in SIRT1 3′ UTR: 5′-UU UUAUAUU-3′; mut sequence: 5′-UUCCCUAUU-3′), respectively. pmut-CPEB1 vector and pmut-SIRT1 vector were constructed, respectively, and the internal parameter was the pRL-TK (E2241; Promega, USA) vector expressing Renilla luciferase. pWT-CPEB1 and pmut-CPEB1 were co-transfected with mimic NC and miR-301 mimic into MCF-7 cells, and pWT-SIRT1 and pmut-SIRT1 were co-transfected with si-NC and si-CPEB1 into MCF-7 cells. The fluorescence intensity was detected at a wavelength 560 nm (firefly relative luminescence unit [RLU]) and wavelength 465 nm (Renilla RLU), according to the Dual Luciferase Reporter Gene Assay Kit (GM-040502A; Qcbio Science &Technologies, Shanghai, PR China), respectively, and the binding intensity was determined by the ratio of firefly RLU/Renilla RLU.

RIPA

The Magna RIP RNA-Binding Protein Immunoprecipitation kit (Millipore, USA) was chosen to reveal the binding of SIRT1 to CPEB1 and then to discard the supernatant after washing with precooled PBS. The cells were lysed with the same volume of RIPA lysate in an ice bath for 5 min, and the supernatant was retained after centrifugation (14,000 rpm, 4°C, 10 min). Part of the cell extract is used as "input," and part of it is co-precipitated with antibody. The steps are as follows: 50 μL of magnetic beads was taken from each co-precipitation reaction system and then re-suspended in 100 μL RIP wash buffer after cleaning. According to different experimental groups, 5 μg of antibodies was added for incubation for binding. After cleaning, the complex of magnetic beads and antibodies was re-suspended in 900 μL RIP wash buffer and incubated overnight at 4°C in 100 μL cell extract. The sample is placed on the magnetic base to collect the magnetic bead-protein complex. Ago2 (ab97051, 1:20,000; Abcam, USA) or CPEB1 antibody (ab181051, 1:5,000; Abcam, USA) should be evenly mixed at room temperature (30 min). In the experiment, IgG acted as a NC, and the experiments were performed three times. The obtained complexes were subjected to RNA purification for qPCR analysis. The primers for miR-301, WT-CPEB1, mut-CPEB1, WT-SIRT1, and mut-SIRT1 were shown in Table S2.

Xenograft tumor in nude mice

In total, 30 female mice (BALB/c, nude mice, 3−7 weeks, 17−23 g) were purchased from Hunan Slac Laboratory Animals (Changsha, Hunan, PR China). These mice were divided into the following four groups randomly: mimic-NC group, miR-301 mimic group, inhibitor-NC group, miR-301 inhibitor group, and miR-301

inhibitor + oe-SIRT1 group. About 1×10^7 prepared cells were inoculated into the armpits of female BALB/c nude mice by subcutaneous inoculation. The width (W) and length (L) of the tumor are measured with calipers every week, and the volume of the tumor was calculated by this formula: $V = (W^2 \times L)/2$. 4 weeks after injection, the mice were euthanized, and the tumor weight was measured. Animal experiments were conducted according to the ethical standards of the animal experiment system approved by the Medical Animal Management Committee of Huashan Hospital, Fudan University.

Immunohistochemistry

After fixed with 10% formaldehyde and embedded in paraffin, the specimens were sliced into 4 μm tissue slices. The tissue slices were baked in an incubator for 1 h (60°C), dewaxed using conventional xylene, dehydrated using gradient alcohol, incubated in 3% H_2O_2 (Sigma) for 30 min (37°C), washed by PBS, boiled in 0.01 M citrate buffer for 20 min (95°C), and rinsed with PBS after cooling to room temperature. Next, the samples were sealed with normal sheep serum (37°C, 10 min) and incubated with primary antibodies, including rabbit anti-CPEB1 (Affinity Biosciences, PR China; DF2462, 1:100), SIRT1 (Affinity Biosciences, PR China; DF6033, 1:100), SOX2 (Affinity Biosciences, PR China; AF5140, 1:100), MCM2 (Abcam; ab108935, 1:2,000), caspase-3 (Affinity Biosciences; AF6311, 1:800), and MMP2 (Affinity Biosciences; AF5330, 1:500) at 4°C for 12 h. The obtained samples were washed with PBS and reacted with the corresponding biotin-labeled second anti-IgG goat anti-rabbit (Affinity Biosciences; S0001, 1:20,000) for 10 min at room temperature. After washing, the horseradish peroxidase-labeled streptomycin working solution was added for reaction for 10 min at room temperature. The sample was developed with DAB, washed with tap water, stained with hematoxylin, dehydrated, cleared, sealed, and finally observed under light microscope. The Japanese Nikon graphic analysis software was used to count the positive cells. Five visual fields with the same area and no repetition were selected for each slice, and the number and proportion of positive cells were calculated. Finally, the average value was calculated, and the experiment was performed three times.

TUNEL assay

The tissue was embedded in paraffin and sliced into 5 μm tissue slices, which were then dewaxed with xylene and alcohol gradient, incubated with protease K (20 μg/mL dissolved in Tris/HCI, pH 7.4∼8.0), and then washed by PBS. The methods referred to the instructions of the TUNEL Apoptosis Detection Kit. The positive staining presented as brownish yellow and was located at the nucleus. Ten high-power visual fields from each section were selected with 200 cells counted in each visual field to calculate the proportion of positive cells and calculate the average value. The experiment was repeated three times.

Statistical analysis

Statistical analysis was conducted with SPSS 21.0 (SPSS, Chicago, IL, USA). The measurement data were described by mean ± standard deviation. Group differences of continuous variables were detected by paired sample t test, independent sample t test, or one-way analysis of variance (ANOVA). Pairwise comparison was tested by Tukey. The cell viability of each group at different time points was compared by two-way ANOVA. Repeated-measures ANOVA was used to compare tumor volumes at multiple time points, with Bonferroni method used for post-test. With median as cutoff value, miR-301 was divided into 2 groups: high expression group and low expression group. The difference of the survival time in different groups was compared by KM. The correlation between CPEB1 and miR-301 was tested by Pearson correlation analysis. Statistical significance was considered as a two-tailed p value < 0.05.

SUPPLEMENTAL INFORMATION

Supplemental information can be found online at https://doi.org/10.1016/j.omto.2021.03.007.

ACKNOWLEDGMENTS

We acknowledge and appreciate our colleagues for their valuable efforts and comments on this paper. The authors confirm that the data supporting the findings of this study are available within the article. This study was supported partly by grants from the Third Batch of Clinical Training Projects of Shenkang (SHDC12019X38).

AUTHOR CONTRIBUTIONS

Y.J. and J.Z. conducted the experiments and designed research. J.Y. prepared figures. J.S. and Z.C. drafted the manuscript. Y.J. edited and revised the manuscript. All authors have approved the final version of manuscript.

DECLARATION OF INTERESTS

The authors declare no competing interests.

REFERENCES

1. Momenimovahed, Z., and Salehiniya, H. (2019). Epidemiological characteristics of and risk factors for breast cancer in the world. Breast Cancer (Dove Med. Press) *11*, 151–164.

2. DeSantis, C.E., Ma, J., Gaudet, M.M., Newman, L.A., Miller, K.D., Goding Sauer, A., Jemal, A., and Siegel, R.L. (2019). Breast cancer statistics, 2019. CA Cancer J. Clin. *69*, 438–451.

3. Li, T., Mello-Thoms, C., and Brennan, P.C. (2016). Descriptive epidemiology of breast cancer in China: incidence, mortality, survival and prevalence. Breast Cancer Res. Treat. *159*, 395–406.

4. Song, Y., Barry, W.T., Seah, D.S., Tung, N.M., Garber, J.E., and Lin, N.U. (2020). Patterns of recurrence and metastasis in BRCA1/BRCA2-associated breast cancers. Cancer *126*, 271–280.

5. Morin, E., Lindskog, C., Johansson, M., Egevad, L., Sandström, P., Harmenberg, U., Claesson-Welsh, L., and Sjöberg, E. (2020). Perivascular Neuropilin-1 expression is an independent marker of improved survival in renal cell carcinoma. J. Pathol. *250*, 387–396.

6. Luo, D., Wilson, J.M., Harvel, N., Liu, J., Pei, L., Huang, S., Hawthorn, L., and Shi, H. (2013). A systematic evaluation of miRNA:mRNA interactions involved in the migration and invasion of breast cancer cells. J. Transl. Med. *11*, 57.

7. Leung, A.K.L. (2015). The Whereabouts of microRNA Actions: Cytoplasm and Beyond. Trends Cell Biol. *25*, 601–610.

8. Qi, Y., Wang, X., Kong, X., Zhai, J., Fang, Y., Guan, X., and Wang, J. (2019). Expression signatures and roles of microRNAs in inflammatory breast cancer. Cancer Cell Int. *19*, 23.

9. Shi, W., Gerster, K., Alajez, N.M., Tsang, J., Waldron, L., Pintilie, M., Hui, A.B., Sykes, J., P'ng, C., Miller, N., et al. (2011). MicroRNA-301 mediates proliferation and invasion in human breast cancer. Cancer Res. *71*, 2926–2937.
10. Qiu, J.J., Lin, X.J., Tang, X.Y., Zheng, T.T., Lin, Y.Y., and Hua, K.Q. (2018). Exosomal Metastasis-Associated Lung Adenocarcinoma Transcript 1 Promotes Angiogenesis and Predicts Poor Prognosis in Epithelial Ovarian Cancer. Int. J. Biol. Sci. *14*, 1960–1973.
11. Nagaoka, K., Fujii, K., Zhang, H., Usuda, K., Watanabe, G., Ivshina, M., and Richter, J.D. (2016). CPEB1 mediates epithelial-to-mesenchyme transition and breast cancer metastasis. Oncogene *35*, 2893–2901.
12. Xu, M., Fang, S., Song, J., Chen, M., Zhang, Q., Weng, Q., Fan, X., Chen, W., Wu, X., Wu, F., et al. (2018). CPEB1 mediates hepatocellular carcinoma cancer stemness and chemoresistance. Cell Death Dis. *9*, 957.
13. Liu, L., Liu, C., Zhang, Q., Shen, J., Zhang, H., Shan, J., Duan, G., Guo, D., Chen, X., Cheng, J., et al. (2016). SIRT1-mediated transcriptional regulation of SOX2 is important for self-renewal of liver cancer stem cells. Hepatology *64*, 814–827.
14. Yoon, D.S., Choi, Y., Jang, Y., Lee, M., Choi, W.J., Kim, S.H., and Lee, J.W. (2014). SIRT1 directly regulates SOX2 to maintain self-renewal and multipotency in bone marrow-derived mesenchymal stem cells. Stem Cells *32*, 3219–3231.
15. Jin, X., Wei, Y., Xu, F., Zhao, M., Dai, K., Shen, R., Yang, S., and Zhang, N. (2018). SIRT1 promotes formation of breast cancer through modulating Akt activity. J. Cancer *9*, 2012–2023.
16. Liu, H., Song, Y., Qiu, H., Liu, Y., Luo, K., Yi, Y., Jiang, G., Lu, M., Zhang, Z., Yin, J., et al. (2020). Downregulation of FOXO3a by DNMT1 promotes breast cancer stem cell properties and tumorigenesis. Cell Death Differ. *27*, 966–983.
17. DeSantis, C., Ma, J., Bryan, L., and Jemal, A. (2014). Breast cancer statistics, 2013. CA Cancer J. Clin. *64*, 52–62.
18. Aggarwal, T., Wadhwa, R., Gupta, R., Paudel, K.R., Collet, T., Chellappan, D.K., Gupta, G., Perumalsamy, H., Mehta, M., Satija, S., et al. (2020). MicroRNAs as Biomarker for Breast Cancer. Endocr. Metab. Immune Disord. Drug Targets *20*, 1597–1610.
19. Stevic, I., Müller, V., Weber, K., Fasching, P.A., Karn, T., Marmé, F., Schem, C., Stickeler, E., Denkert, C., van Mackelenbergh, M., et al. (2018). Specific microRNA signatures in exosomes of triple-negative and HER2-positive breast cancer patients undergoing neoadjuvant therapy within the GeparSixto trial. BMC Med. *16*, 179.
20. Cui, L., Li, Y., Lv, X., Li, J., Wang, X., Lei, Z., and Li, X. (2016). Expression of MicroRNA-301a and its Functional Roles in Malignant Melanoma. Cell. Physiol. Biochem. *40*, 230–244.
21. Fujita, Y., Masuda, K., Hamada, J., Shoda, K., Naruto, T., Hamada, S., Miyakami, Y., Kohmoto, T., Watanabe, M., Takahashi, R., et al. (2017). KH-type splicing regulatory protein is involved in esophageal squamous cell carcinoma progression. Oncotarget *8*, 101130–101145.
22. Silva, J., García, V., Zaballos, Á., Provencio, M., Lombardía, L., Almonacid, L., García, J.M., Domínguez, G., Peña, C., Diaz, R., et al. (2011). Vesicle-related microRNAs in plasma of nonsmall cell lung cancer patients and correlation with survival. Eur. Respir. J. *37*, 617–623.
23. Fan, H., Jin, X., Liao, C., Qiao, L., and Zhao, W. (2019). MicroRNA-301b-3p accelerates the growth of gastric cancer cells by targeting zinc finger and BTB domain containing 4. Pathol. Res. Pract. *215*, 152667.
24. Fernández-Miranda, G., and Méndez, R. (2012). The CPEB-family of proteins, translational control in senescence and cancer. Ageing Res. Rev. *11*, 460–472.
25. Luong, X.G., Daldello, E.M., Rajkovic, G., Yang, C.R., and Conti, M. (2020). Genome-wide analysis reveals a switch in the translational program upon oocyte meiotic resumption. Nucleic Acids Res. *48*, 3257–3276.
26. Xiong, H., Chen, R., Liu, S., Lin, Q., Chen, H., and Jiang, Q. (2018). MicroRNA-183 induces epithelial-mesenchymal transition and promotes endometrial cancer cell migration and invasion in by targeting CPEB1. J. Cell. Biochem. *119*, 8123–8137.
27. Shoshan, E., Mobley, A.K., Braeuer, R.R., Kamiya, T., Huang, L., Vasquez, M.E., Salameh, A., Lee, H.J., Kim, S.J., Ivan, C., et al. (2015). Reduced adenosine-to-inosine miR-455-5p editing promotes melanoma growth and metastasis. Nat. Cell Biol. *17*, 311–321.
28. Yin, J., Park, G., Lee, J.E., Park, J.Y., Kim, T.H., Kim, Y.J., Lee, S.H., Yoo, H., Kim, J.H., and Park, J.B. (2014). CPEB1 modulates differentiation of glioma stem cells via down-regulation of HES1 and SIRT1 expression. Oncotarget *5*, 6756–6769.
29. Wilking, M.J., and Ahmad, N. (2015). The role of SIRT1 in cancer: the saga continues. Am. J. Pathol. *185*, 26–28.
30. Deng, C.X. (2009). SIRT1, is it a tumor promoter or tumor suppressor? Int. J. Biol. Sci. *5*, 147–152.
31. Wang, R.H., Sengupta, K., Li, C., Kim, H.S., Cao, L., Xiao, C., Kim, S., Xu, X., Zheng, Y., Chilton, B., et al. (2008). Impaired DNA damage response, genome instability, and tumorigenesis in SIRT1 mutant mice. Cancer Cell *14*, 312–323.
32. Karbasforooshan, H., Roohbakhsh, A., and Karimi, G. (2018). SIRT1 and microRNAs: The role in breast, lung and prostate cancers. Exp. Cell Res. *367*, 1–6.
33. Saunders, L.R., and Verdin, E. (2007). Sirtuins: critical regulators at the crossroads between cancer and aging. Oncogene *26*, 5489–5504.
34. Iturri, J., Weber, A., Vivanco, M.D., and Toca-Herrera, J.L. (2020). Single-Cell Probe Force Studies to Identify Sox2 Overexpression-Promoted Cell Adhesion in MCF7 Breast Cancer Cells. Cells *9*, 935.